Chinese Chemical Letters 33 (2022) 1637–1642

Contents lists available at ScienceDirect

Chinese Chemical Letters

journal homepage: www.elsevier.com/locate/cclet

High-contrast and real-time visualization of membrane proteins in live cells with malachite green-based fluorogenic probes

Yefeng Chen[1], Chenghong Xue[1], Jie Wang[1], Minqiu Xu, Yuyao Li, Yiru Ding, Heng Song, Weipan Xu, Hexin Xie*

State Key Laboratory of Bioreactor Engineering, Shanghai Key Laboratory of New Drug Design, Frontiers Science Center for Materiobiology and Dynamic Chemistry, School of Pharmacy, East China University of Science and Technology, Shanghai 200237, China

ARTICLE INFO

Article history:
Received 8 July 2021
Revised 19 September 2021
Accepted 24 September 2021
Available online 30 September 2021

Keywords:
Cellular imaging
Fluorogenic probe
Environment-sensitive fluorophore
Alkaline phosphatase
Integrin

ABSTRACT

Imaging dynamics of membrane proteins of live cells in a wash-free and real-time manner has been a challenging task. Herein, we report unprecedented applications of malachite green (MG), an organic dye widely used in pigment industry, as a switchable fluorophore to monitor membrane enzymes or non-catalytic proteins in live cells. Conformationally flexible MG is non-fluorescent in aqueous solution, yet covalent binding with endogenous proteins of cells significantly enhances its fluorescence at 670 nm by restricting flexibility of dye. Integrating a phosphate-caged quinone methide precursor with MG yielded a covalent labeling fluorogenic probe, allowing real-time imaging of membrane alkaline phosphatase (ALP, a model catalytic protein) activity in live cells with over 100-fold enhancement of fluorescence intensity. Moreover, MG is also applicable to image non-catalytic protein by conjugation with protein-specific ligand. A fluorogenic probe consisted of *c*-RGDfK peptide and MG proved to be compatible with wash-free and real-time visualization of non-catalytic integrin $\alpha_v\beta_3$ in live cells with high contrast.

Membrane proteins, including catalytic and non-catalytic proteins, play critical roles in a vast diverse of biological processes in life. Specific visualization or detection of these proteins is of high importance in the investigations of sophisticated functions of these macromolecules in biological processes and even diagnosis of disease. Small-molecule fluorescent probes have emerged as powerful tools to non-invasively image proteins, particularly catalytic proteins (*i.e.*, enzymes), in their native environments [1–11]. Currently, most of these activatable fluorescent probes are based on the activities of enzymes, which convert non-fluorescent substrates into fluorescent molecules or lead to the change of emission wavelength.

Nevertheless, membrane enzymes are in a highly dynamic environment. Majority of these fluorescent reagents, despite high fluorescence quantum yield in homogenous aqueous solution upon activation by enzyme, inevitably suffer from rapid diffusion of activated fluorophores. To address this challenge, a number of trappable fluorogenic probes have been developed. Well-known examples include aggregation-induced emission (AIE)-based probes [12–15], which stay at sites of activation by precipitation and enhance fluorescence intensity upon interaction with target enzymes. This strategy has been widely applied to image activity of membrane alkaline phosphatase (ALP) in live cells [16–20]. Ye and co-workers took advantage of the enzyme-instructed self-assembly strategy [21] to develop a near-infrared (NIR) fluorogenic probe to visualize endogenous ALP on outer membranes of live cells [22]. Very recently, our lab integrated quinone methide (QM) with fluorogenic probe to construct a number of covalently trappable fluorescent reagents for the real-time imaging of activity of membrane enzymes, including ALP [23] and γ-glutamyl transpeptidase (GGT) [24].

On the other hand, the imaging of non-catalytic protein typically relies on always-on fluorescent reagents, which makes it a challenging task to visualize proteins in real time as a washing step is needed to remove unbound fluorescent probes. In recent years, a number of environment-sensitive fluorophores, such as naphthalimide, dansyl, nitrobenzoxadiazole (NBD), and their derivatives, have been incorporated with protein-specific ligands to image non-catalytic proteins [25,26]. These probes usually are weakly fluorescent in aqueous medium but turn strong fluorescent upon interaction with target proteins due to the change of surrounding environment. Notably, some of the AIE-based fluorophores are reported to be sensitive to surrounding environment and these fluorophores have been explored in the detection of non-catalytic proteins in

* Corresponding author.
E-mail address: xiehexin@ecust.edu.cn (H. Xie).
[1] These authors contributed equally to this work.

https://doi.org/10.1016/j.cclet.2021.09.088
1001-8417/

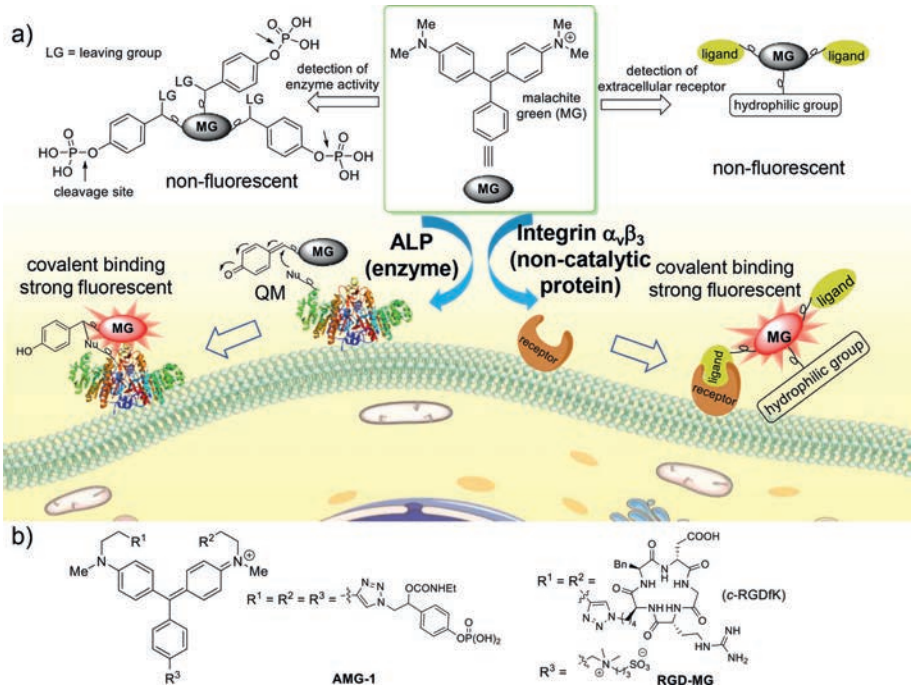

Fig. 1. (a) Schematic illustration of imaging of extracellular catalytic or non-catalytic proteins in live cells with MG-based fluorogenic probes. (b) Chemical structures of MG-based probes in this study.

live cells [27]. In 2018, the Tan's lab developed a fluorescence-switchable NIR fluorophore, P-Mero4, which can be applied in the wash-free imaging of intracellular non-catalytic proteins in live cells [28]. Recently, Urano and co-workers demonstrated Si-rhodamine could be used as an environment-sensitive dye to visualize membrane folate receptor in live cells [29]. However, in spite of these encouraging results, the employment of these fluorophores in real-time and wash-free imaging of dynamics of biologically important proteins in lives cells may still face one or even more challenges, including low photostability, synthetic difficulty, and low signal-to-background ratio (SBR). A desirable fluorescence probe that is compatible with real-time imaging of membrane proteins in live cells should: (1) selectively trap at or around target protein; (2) significantly increase fluorescence intensity or shift emission wavelength upon interaction with target protein; (3) has high photostability to allow long-term visualization of cells.

Malachite green (MG) is an organic dye widely used in dyestuff industry and pigment industry. This molecule, though with high structural similarity as widely used fluorophore tetramethylrhodamine (TMR), has been largely excluded as a fluorescent reporter in cell imaging because of its extremely low fluorescence quantum yield in aqueous solution. However, cellular environment is dramatically different from homogenous aqueous solution. The low fluorescence emission of MG in solution, along with its high environmental sensitivity, may be advantageous in live cell imaging, especially in visualization of membrane proteins; it efficiently reduces background fluorescence signal and thus allows washing-free and real-time imaging of cellular targets. Herein, upon incorporation with covalent labeling strategy, we report unprecedented applications of MG as an activatable near-infrared fluorophore in wash-free and real-time visualization of endogenous membrane proteins, including catalytic proteins and non-catalytic proteins, with up to over 100-fold of fluorescence enhancement ratio and 200-fold of signal-to-background ratio in live cells. The merits of these MG-based probes also include high photostability and easy synthesis.

MG is non-fluorescent in aqueous solution because of its high conformation flexibility. Previous investigations have indicated that restricting vibration of MG by cold or viscous environment [30,31], aptamers [32–34], or selected proteins that have high affinity to MG [35–37] significantly enhanced its fluorescence. Inspired by these studies, we envisaged selectively labeling this molecule to target proteins or nearby proteins in a covalent manner might efficiently reduce its conformation flexibility and thus lead to enhancement of fluorescence signal. With this label-and-emission strategy, MG may offer unique opportunity to allow wash-free and real-time imaging of endogenous membrane proteins in live cells.

To test the feasibility of this hypothesis, we selected biologically important ALP [38–41] as a catalytic model protein and integrin $\alpha_v\beta_3$ [42–44] as a non-catalytic model protein, both of which are mainly found on outer membrane of cells. As shown in Fig. 1, to construct a MG-based fluorescent probe, AMG-1, for the detection of ALP activity in live cells, we installed three phosphate-caged quinone methide (QM) [45–48] precursors on MG. The hydrolysis AMG-1 by ALP releases highly reactive QM intermediate, which then reacts with nucleophilic residue from ALP or nearby proteins. The covalent immobilization of MG in cells might effectively restrict conformation flexibility of MG and thus turns on fluorescence signal. The fluorescence probe for integrin $\alpha_v\beta_3$, RGD-MG, consists of three parts: cyclic peptide *c*-RGDfK (as a recognition unit), MG dye (as a fluorescent reporter), and a zwitterion (as a hydrophilic group). Similarly, specific binding of *c*-RGDfK to integrin $\alpha_v\beta_3$ may lead to significant fluorescence enhancement of MG.

These fluorogenic probes, AMG-1 and RGD-MG, were readily prepared by assembling alkynyl-substituted MG with azido-containing phosphate-caged quinone methide precursor or *c*-RGDfK by a CuAAC click reaction (Scheme S1 in Supporting information) [49]. This approach should allow rapid synthesis of a variety of MG-based fluorescence probes.

With AMG-1 in hand, we commenced to investigate its photophysical and chemical properties in homogeneous aqueous solution. The change of AMG-1 in fluorescence intensity before and

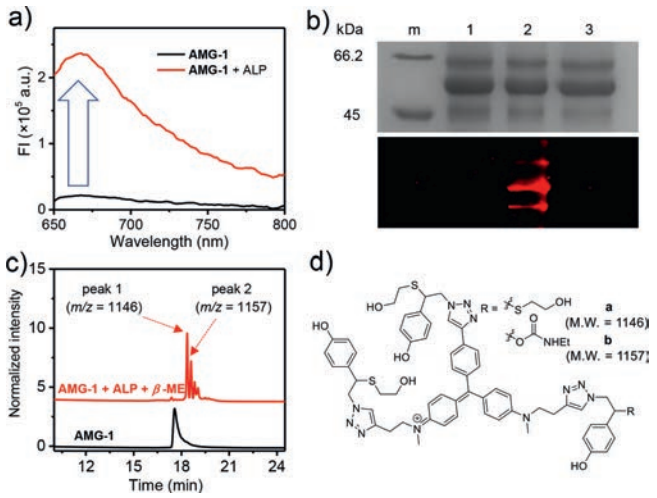

Fig. 2. *In vitro* characterization of MG-based probe AMG-1. (a) Fluorescence spectra of AMG-1 (10 μmol/L in PBS) before and after incubation with ALP (30 U/mL) at 37 °C for 2 h. (b) Coomassie blue staining (top) and fluorescence (bottom) images of SDS-PAGE gel. ALP was incubated with AMG-1 in the presence or absence of Na_3VO_4 (ALP inhibitor) in PBS at 37 °C for 2 h before PAGE analysis. m: protein marker; (1): ALP; (2): ALP + AMG-1; (3): ALP + AMG-1 + Na_3VO_4. (c) HPLC and mass spectra analysis of AMG-1 (10 μmol/L) upon incubation with ALP (2 U/mL) and β-ME (10 mmol/L) at 37 °C for 2 h. (d) Chemical structures of plausible products.

after incubation of ALP was first recorded (Fig. 2a). As expected, AMG-1 in phosphate-buffered saline (PBS, pH 7.4) alone exhibited very low fluorescence intensity, while the addition of ALP increased the fluorescence of AMG-1 for about 10 folds. Nevertheless, cellular environment may differ from homogenous aqueous solution and leads to even higher fluorescence enhancement ratio of AMG-1.

To gain further information on the ALP-triggered labeling process of AMG-1, we used β-mercaptoethanol (β-ME) as external nucleophile to mimic possible nucleophilic residue of proteins. After incubation of AMG-1 with ALP in the presence of excess amount of β-ME for 2 h, we analyzed the reaction mixture using high performance liquid chromatography (HPLC). As can be seen from Fig. 2c, probe AMG-1 has been hydrolyzed by ALP completely, leaving two compounds (peaks 1 and 2) as major products. The structures of these two compounds were further confirmed to be adducts of quinone methide intermediate with two (*b*) and three β-MEs (*a*) (Fig. 2d) by liquid chromatography-mass spectrometry (LC-MS). Moreover, the minor components observed from the HPLC trace are likely resulted from the nucleophilic addition of quinone methide intermediate by one β-ME or different number of other nucleophiles (*e.g.*, water). The identification of these products confirms the formation of highly electrophilic quinone methide intermediate after hydrolysis by ALP and suggests probe AMG-1 may have multiple opportunities to be covalently labeled by enzyme or proteins.

To further validate the formation of covalent bond with ALP, we analyzed the probe-incubated ALP using in-gel fluorescence imaging. As shown in Fig. 2b. We observed obvious NIR fluorescence signal from band of ALP, manifesting this enzyme was effectively labeled by AMG-1. Moreover, dramatic reduction of fluorescence on ALP by the addition of ALP inhibitor, Na_3VO_4, indicates the observed fluorescence signal on ALP is indeed originated from the hydrolysis of AMG-1 by enzyme.

Photobleaching of fluorophore is a significant problem in fluorescence imaging of live cells and some of the environment-sensitive fluorophores suffer a lot from low photostability. To assess the photostability of MG-based probe, we placed a solution of AMG-1 on a fluorescence microscope with continuous irradiation at 604–644 nm and monitored its time-course fluorescence intensity. As shown in Fig. S1 (Supporting information), fluorescence intensity of AMG-1 remained unchanged over a period of 10 min under high-intensity illumination. As a comparison, the fluorescence intensity of an ALP-labeling probe ALP NIR-1 [48], which used environment-sensitive P-Mero4 [28] as a NIR fluorophore, diminished rapidly under identical experimental conditions. These results demonstrate the high photostability of MG-based probe, which is of particular importance in real-time and continuous imaging of live cells.

Encouraged by these results, we then moved to investigate this MG-based reagent in live cells. Cytotoxicity of AMG-1 was first investigated with standard MTT assay (Fig. S2 in Supporting information). After incubation a variety concentrations of AMG-1 with HeLa cells or HEK 293 cells, we observed no significant impact on the viability of cells at up to 30 μmol/L, suggesting this reagent is compatible with mammalian cells.

To probe whether AMG-1 is suitable to image ALP activity in live cells, we simply incubated this molecule with HeLa cells or HEK 293 cells for 2 h and then acquired fluorescence images with confocal microscope without a washing step (Fig. 3a). These images showed that ALP-overexpressing HeLa cells fluoresced intensively whereas ALP-negative HEK 293 cells remained fluorescently silent under identical conditions. Moreover, the fluorescence signal stayed exclusively on membrane of HeLa cells, on which ALP is mainly located [50]. Pretreating HeLa cells with 10 mmol/L of Na_3VO_4, an ALP inhibitor, for 1 h before incubation with AMG-1 significantly suppressed fluorescence on HeLa cells, manifesting the observed fluorescence signal was specific to the activity of ALP.

Besides HeLa cells, we also tested ALP-overexpressing HepG2 cells and HCT116 cells with AMG-1 and comparable results were obtained: Membrane of these cells was markedly fluorescent while inhibition of ALP activity of cells by pretreating cells with inhibitor resulted in significantly reduced fluorescence (Fig. 3a).

To further confirm the observed fluorescence in cells precisely represented the activity of ALP in cells, we quantified the fluorescence intensity on HeLa cells and HEK 293 cells, respectively (Fig. 3b). It turned out the average fluorescence intensity of HeLa cells was 57 folds stronger than that of HEK 293 cells. These results are consistent with the relative ALP activity measured in lysate of a large number of cells with a fluorogenic umbelliferyl phosphate as a substrate (57 *vs.* 60 folds, Fig. 3c and Fig. S3 in Supporting information), demonstrating this MG-based probe could be used as a reliable and convenient reagent to measure membrane ALP activity of live cells.

Unlike most of the other fluorogenic enzyme substrates, the covalent labeling ability of AMG-1 should allow selective labeling of ALP-overexpressing cells even in the presence of negative cells. To test this possibility, we incubated a mixture of HeLa cells and HEK 293 cells with AMG-1 and analyzed labeling specificity with microscope. As shown in Fig. S4 (Supporting information), we only observed strong fluorescence from ALP-overexpressing HeLa cells with ALP-negative HEK 293 cells basically non-fluorescent. The excellent labeling specificity of AMG-1 would be of high importance in the identification of enzyme activity in complicated biological environments.

TG-Phos is a Tokyo Green-based fluorogenic substrate of ALP with high fluorescence turn-on ratio and quantum yield in homogenous aqueous solution upon enzymatic hydrolysis [51]. However, incubation of this probe with a mixture of HeLa cells and HEK 293 cells resulted in fluorescence signal on both types of cells, ALP-negative HEK 293 cells and ALP-overexpressing HeLa cells (Fig. 4). The fluorescence on cells was only marginally stronger than background signal, in spite of high fluorescence turn-on ratio and quantum yield of this probe. Fluorescence signal appeared to emit from inside of cells, instead of exclusive membrane of ALP-

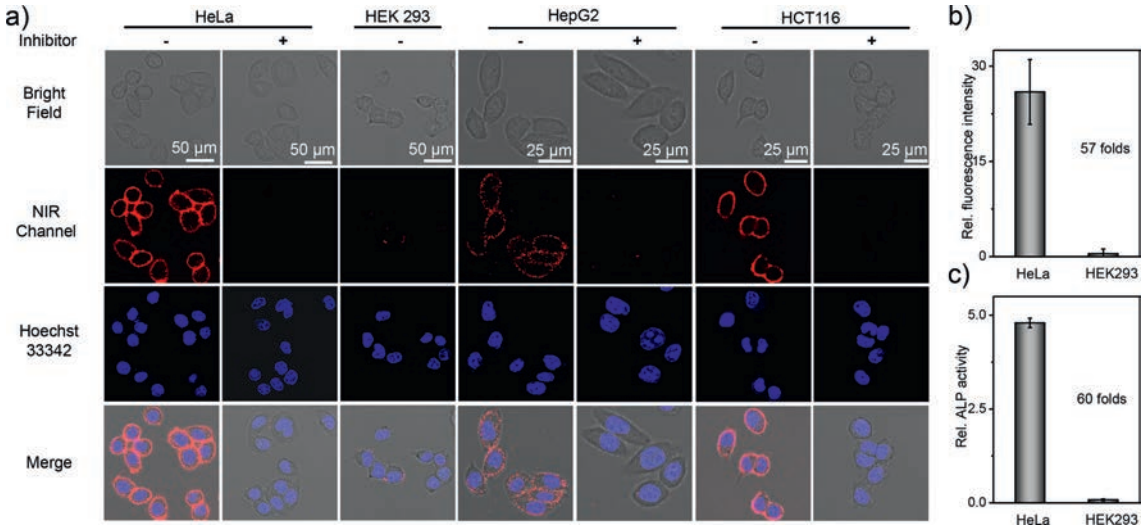

Fig. 3. (a) Imaging of extracellular ALP activity in live cells with MG-based probe AMG-1. (a) Confocal fluorescence imaging of HeLa cells, HEK 293 cells, HepG2 cells, and HCT116 cells with AMG-1. AMG-1 (5 μmol/L) was incubated at 37 °C for 2 h with indicated cells, as well as cells pretreated with Na_3VO_4 (5 mmol/L, inhibitor of ALP) for 1 h. (b) Average fluorescence intensity at NIR channel on HeLa cells and HEK 293 cells in (a). Error bars were calculated on N measurements with N = 14 and 8. (c) ALP activity of lysated HeLa cells and HEK 293 cells determined by fluorogenic enzyme substrate (see Fig. S3 for details). λ_{ex} = 633 nm, λ_{em} = 655–685 nm. Data are the average of three replicate experiments. Error bars are ± s.d.

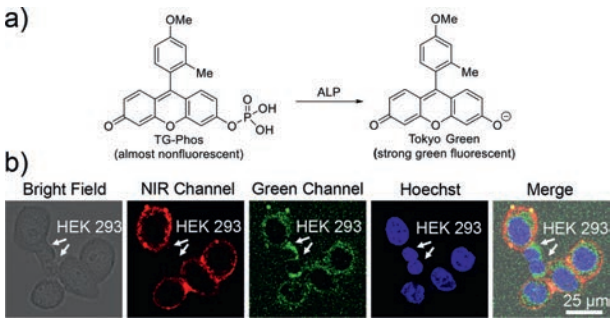

Fig. 4. Specific labeling of ALP-overexpressing HeLa cells in the presence of negative HEK 293 cells. (a) Fluorescence turn-on of green fluorogenic probe TG-Phos by ALP. (b) Confocal fluorescence imaging of HeLa cells and HEK 293 cells after incubation with TG-Phos and AMG-1 subsequently. A mixture of HeLa cells and HEK 293 cells were incubated with TG-Phos (20 μmol/L) at 37 °C for 2 h, followed by washing with PBS and incubation with AMG-1 (5 μmol/L) at 37 °C for 2 h. NIR channel: λ_{ex} = 633 nm, λ_{em} = 655–685 nm; Green channel: λ_{ex} = 488 nm, λ_{em} = 500–520 nm.

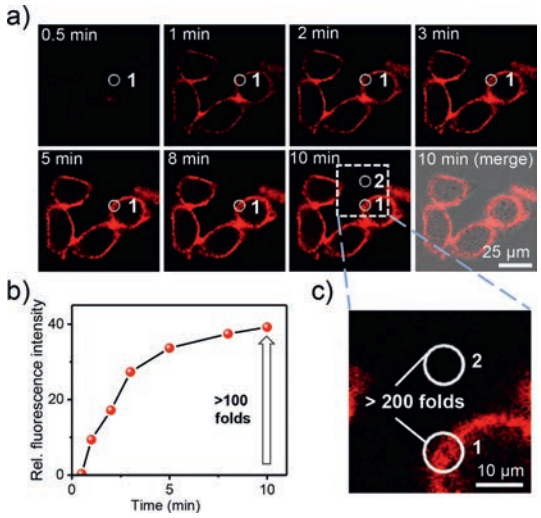

Fig. 5. Wash-free and real-time imaging of extracellular ALP activity in live HeLa cells with MG-based probe AMG-1. (a) Time-course confocal fluorescence imaging of HeLa cells incubated with AMG-1 (0.8 μmol/L). (b) Time-course fluorescence intensity of circle 1 in (a). (c) Amplified fluorescence image at 10 min. λ_{ex} = 633 nm, λ_{em} = 655–685 nm.

overexpressing cells as AMG-1. And a washing step was required to remove free fluorophore in medium before imaging with microscope. Similar results were obtained when a coumarin-based fluorogenic probe, umbelliferyl phosphate [52], was used (Fig. S5 in Supporting information). The poor efficiency of these fluorogenic probes in live cells imaging is apparently due to low retention of activated fluorophores in cells. In sharp contrast, covalently labeling ability of AMG-1 led to not only accumulation of MG selectively on ALP-overexpressing cells but also enhancement of fluorescence by restriction of flexibility, and thus yielded much higher SBR and specificity even though MG has much lower fluorescence quantum yield in solution compared to Tokyo Green or umbelliferone.

Prompted by the high photostability and compatibility of AMG-1 with wash-free visualization of cells, we proceeded to investigate whether this reagent can be used in real-time imaging of enzyme activity in live cells. We treated HeLa cells with AMG-1 and then monitored fluorescence of cells immediately with confocal fluorescence microscope without a wash step. As shown in Fig. 5, only 1 MIM after incubation, obvious NIR fluorescence signal appeared on membrane of HeLa cells. The fluorescence on cell membrane increased constantly over time until reaching a plateau in about 10 min. We detected more than 100-fold enhancement of fluorescence on cell membrane compared to the one incubated for 30 s. The fluorescence increasement ratio on cells could be even higher as the fluorescence image of cells at time zero was unable to capture. It is worth noting that the fluorescence enhancement ratio of AMG-1 on cell membrane is significantly higher than that of solution-based test (> 100 *vs.* 10 folds). We reasoned the high fluorescence turn-on ratio on cells may be due to (1) higher efficiency of proteins on cell membrane to restrict flexibility of MG compared to those in solution; (2) accumulation of MG-based probe on cell membrane.

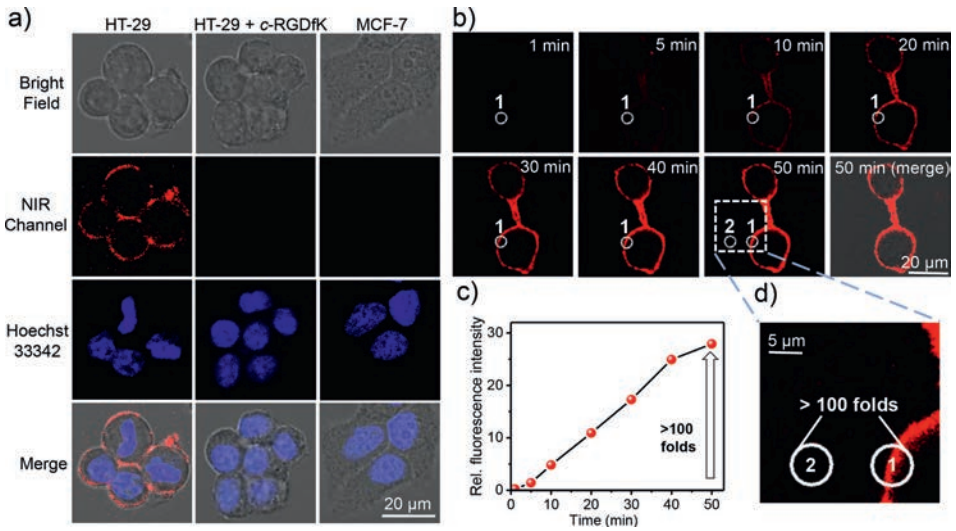

Fig. 6. (a) Imaging of integrin $\alpha_v\beta_3$ in live cells with MG-based probe RGD-MG. (a) Confocal fluorescence imaging of HT-29 cells and MCF-7 cells with probe. RGD-MG (2 μmol/L) was incubated at 4 °C for 1 h with the indicated cells or cells pretreated with c-RGDfK (100 μmol/L) for 0.5 h. (b) Real-time confocal fluorescence imaging of HT-29 cells incubated with RGD-MG (2 μmol/L) at 4 °C. (c) Time-course fluorescence intensity of circle 1 in (b). (d) Amplified fluorescence image of HT-29 cells at 50 min. λ_{ex} = 633 nm, λ_{em} = 655-685 nm.

SBR is among the most important criteria for fluorescence imaging of cells. We randomly compared the fluorescence signal on cell membrane with background signal at 10 min of incubation and the ratio turned out to be over 200 folds (Fig. 5c). This is particularly impressed given the fact that no wash step was involved in this study. The exceptionally high SBR likely is beneficial from the extremely low fluorescence quantum yield of MG in solution.

MG-based AMG-1 relies on ALP-triggered immobilization to report enzyme activity in live cells. The unique label-and-emission feature of MG, besides catalytic proteins, may also be valuable in the imaging of membrane non-catalytic proteins in live cells. Integrin $\alpha_v\beta_3$ is a type of outer membrane-bounded protein that regulates the grown and metastasis of tumor and thus has been considered as an important biomarker for early diagnosis of solid tumors [44]. To test whether a MG-based probe is capable of imaging integrin $\alpha_v\beta_3$ in live cells, a MG-based probe, RGD-MG, has been prepared, which uses a *c*-RGDfK peptide as specific ligand for integrin $\alpha_v\beta_3$. The cytotoxicity of RGD-MG against HT-29 cells and MCF-7 cells was evaluated with standard MTT assay, which proved this probe is highly compatible to HT-29 cells and MCF-7 cells even at concentration of up to 30 μmol/L (Fig. S6 in Supporting information).

We then incubated integrin $\alpha_v\beta_3$-overexpressing HT-29 cells with MG-based probe RGD-MG for 1 h at 4 °C and acquired its fluorescence image with confocal microscope without washing away free probe. As shown in Fig. 6a, we observed strong NIR fluorescence specifically from membrane of HT-29 cells, where integrin $\alpha_v\beta_3$ is mainly located. Pretreating HT-29 cells with *c*-RGDfK peptide before incubation with RGD-MG efficiently blocked the emission of fluorescence from HT-29 cells, indicating the observed fluorescence signal on HT-29 cells is specifically resulted from interaction of integrin $\alpha_v\beta_3$ with RGD-MG. The incubation of integrin $\alpha_v\beta_3$-negative MCF-7 cells with RGD-MG under identical experiment conditions led to significantly less fluorescence signal on cell membrane, demonstrating this MG-based probe can readily discriminate integrin $\alpha_v\beta_3$-overexpressing cells from negative cells.

Taking advantage of the label-and-emission feature of MG, probe RGD-MG should be compatible with real-time imaging of integrin $\alpha_v\beta_3$ in live cells. To investigate this, we incubated HT-29 cells with RGD-MG at 4 °C and monitored with microscope immediately. As shown in Fig. 6b, culture medium and cells were completely dark at the beginning. As incubation time elapsed, the fluorescence intensity on membrane of cells increased gradually while the background remained non-fluorescent, indicating probe RGD-MG continuously bound with integrin $\alpha_v\beta_3$ of HT-29 cells. The fluorescence intensity of a single spot of membrane enhanced over 100 folds from 1 min of incubation to 50 min (Fig. 6c). More significantly, the SBR of cellular image at 50 min of incubation is over 100 folds (Fig. 6d). These results show MG has great potential not only in visualization of membrane enzyme activity but also in real-time tracking of non-catalytic proteins in live cells.

In summary, we have demonstrated unprecedented applications of readily available malachite green as a switchable fluorophore to visualize endogenous membrane proteins in live cells. This conformationally flexible organic dye is non-fluorescent in homogeneous aqueous solution but emits strong fluorescence at 670 nm upon restriction of conformation flexibility by covalent binding with proteins of cells. With malachite green as a fluorescent reporter, we have shown a quinone methide-based covalent labeling probe, AMG-1, was suitable for wash-free and real-time imaging of membrane alkaline phosphatase in live cells with high fluorescence turn-on ratio (> 100 folds) and signal-to-background ratio (> 100 folds). This probe proved to be able to selectively label ALP-overexpressing cells in the presence of negative cells. Moreover, taking advantage of the label-and-emission characteristic, malachite green is also compatible with no-wash and real-time visualization of non-catalytic integrin $\alpha_v\beta_3$ in live cells. The merits of malachite green-based probe are further underscored by high photostability and easy synthesis. Upon integration with the covalent labeling strategy, malachite green should find greater value in the imaging of dynamic of other membrane proteins both catalytic proteins and non-catalytic proteins in live cells.

Declaration of competing interest

The authors declare that they have no known competing financial interests or personal relationships that could have appeared to influence the work reported in this paper.

Acknowledgments

This study was financially supported by the National Natural Science Foundation of China (No. 22077031), the Research Program of State Key Laboratory of Bioreactor Engineering, and the Fundamental Research Funds for the Central Universities.

Supplementary materials

Supplementary material associated with this article can be found, in the online version, at doi:10.1016/j.cclet.2021.09.088.

References

[1] A. Razgulin, N. Ma, J. Rao, Chem. Soc. Rev. 40 (2011) 4186.
[2] R. Yan, D. Ye, Sci. Bull. 61 (2016) 1672–1679.
[3] W. Chyan, R.T. Raines, ACS Chem. Biol. 13 (2018) 1810–1823.
[4] H. Liu, L. Chen, C. Xu, et al., Chem. Soc. Rev. 47 (2018) 7140–7180.
[5] K. Singh, A.M. Rotaru, A.A. Beharry, ACS Chem. Biol. 13 (2018) 1785–1798.
[6] J. Zhang, X. Chai, X.P. He, et al., Chem. Soc. Rev. 48 (2019) 683.
[7] X. Wu, W. Shi, X. Li, H. Ma, Acc. Chem. Res. 52 (2019) 1892–1904.
[8] W. Qin, C. Xu, Y. Zhao, et al., Chin. Chem. Lett. 29 (2018) 1451–1455.
[9] D. Chen, W. Qin, H. Fang, et al., Chin. Chem. Lett. 30 (2019) 1738–1744.
[10] F. Song, R. Liang, J. Deng, Z. Liu, X. Peng, Chin. Chem. Lett. 28 (2017) 1997–2000.
[11] Z. Li, X. Xia, Y. You, et al., Chin. Chem. Lett. 32 (2021) 1785–1789.
[12] J. Luo, Z. Xie, J.W. Lam, et al., Chem. Commun. (2001) 1740–1741.
[13] Y.N. Hong, J.W.Y. Lam, B.Z. Tang, Chem. Soc. Rev. 40 (2011) 5361–5388.
[14] J. Mei, Y. Hong, J.W. Lam, et al., Adv. Mater. 26 (2014) 5429–5479.
[15] J. Mei, N.L. Leung, R.T. Kwok, J.W. Lam, B.Z. Tang, Chem. Rev. 115 (2015) 11718–11940.
[16] H.W. Liu, K. Li, X.X. Hu, et al., Angew. Chem. Int. Ed. 56 (2017) 11788–11792.
[17] X. Gu, G. Zhang, Z. Wang, et al., Analyst 138 (2013) 2427–2431.
[18] J. Liang, R.T. Kwok, H. Shi, B.Z. Tang, B. Liu, ACS Appl Mater Interfaces 5 (2013) 8784–8789.
[19] M. Zhao, Y. Gao, S. Ye, et al., Analyst 144 (2019) 6262–6269.
[20] H. Li, Q. Yao, F. Xu, et al., Angew. Chem. Int. Ed. 59 (2020) 10186–10195.
[21] B.J. Kim, B. Xu, Bioconjug. Chem. 31 (2020) 492–500.
[22] R. Yan, Y. Hu, F. Liu, et al., J. Am. Chem. Soc. 141 (2019) 10331–10341.
[23] Y. Li, H. Song, C. Xue, et al., Chem. Sci. 11 (2020) 5889–5894.
[24] Y. Li, C. Xue, Z. Fang, W. Xu, H. Xie, Anal. Chem. 92 (2020) 15017–15024.
[25] Z. Liu, L. Du, M. Li, Sci. China Chem. 56 (2013) 1667–1670.
[26] Y.D. Zhuang, P.Y. Chiang, C.W. Wang, K.T. Tan, Angew. Chem. Int. Ed. 52 (2013) 8124–8128.
[27] H.B. Shi, J.Z. Liu, J.L. Geng, B.Z. Tang, B. Liu, J. Am. Chem. Soc. 134 (2012) 9569–9572.
[28] H.J. Chen, C.Y. Chew, E.H. Chang, et al., J. Am. Chem. Soc. 140 (2018) 5224–5234.
[29] K. Numasawa, K. Hanaoka, N. Saito, et al., Angew. Chem. Int. Ed. 59 (2020) 6015–6020.
[30] G. Oster, Y. Nishijima, J. Am. Chem. Soc. 78 (1956) 1581–1584.
[31] S.B. Baptista, G.L. Indig, J. Phys. Chem. B 102 (1998) 4678–4688.
[32] J.R. Babendure, S.R. Adams, R.Y. Tsien, J. Am. Chem. Soc. 125 (2003) 14716–14717.
[33] D.M. Kolpashchikov, J. Am. Chem. Soc. 127 (2005) 12442–12443.
[34] W.C. Xu, Y. Lu, Anal. Chem. 82 (2010) 574–578.
[35] C. Szent-Gyorgyi, B.F. Schmidt, Y. Creeger, et al., Nat. Biotechnol. 26 (2008) 235–240.
[36] C.P. Pratt, J. He, Y. Wang, A.L. Barth, M.P. Bruchez, Bioconjug. Chem. 26 (2015) 1963–1971.
[37] C.A. Telmer, R. Verma, H. Teng, et al., ACS Chem. Biol. 10 (2015) 1239–1246.
[38] J.L. Millan, W.H. Fishman, Crit. Rev. Clin. Lab. Sci. 32 (1995) 1–39.
[39] N.K. Tonks, Nat. Rev. Mol. Cell Biol. 7 (2006) 833–846.
[40] R.B. McComb, G.N. Bowers Jr., S. Posen, Plenum Publishing Corporation, New York, 2013.
[41] C. Liu, S. Yang, Y. Qiao, et al., Chin. Chem. Lett. 32 (2021) 1809–1813.
[42] A. van der Flier, A. Sonnenberg, Cell Tissue Res 305 (2001) 285–298.
[43] B. Felding-Habermann, Clin. Exp. Metastasis 20 (2003) 203–213.
[44] G.H. Mahabeleshwar, W. Feng, D.R. Phillips, T.V. Byzova, J. Exp. Med. 203 (2006) 2495–2507.
[45] S. Halazy, V. Berges, A. Ehrhard, C. Danzin, Bioorg. Chem. 18 (1990) 330–344.
[46] J.K. Myers, T.S. Widlanski, Science 262 (1993) 1451–1453.
[47] S.E. Rokita, Wiley, Hoboken, New York, 2009.
[48] H. Song, Y. Li, Y. Chen, C. Xue, H. Xie, Chem. Eur. J. 25 (2019) 13994–14002.
[49] H.C. Kolb, M.G. Finn, K.B. Sharpless, Angew. Chem. Int. Ed. 40 (2001) 2004–2021.
[50] C.W. Lin, M. Sasaki, M.L. Orcutt, H. Miyayama, R.M. Singer, J. Histochem. Cytochem. 24 (1976) 659–667.
[51] M. Kamiya, Y. Urano, N. Ebata, et al., Angew. Chem. Int. Ed. 44 (2005) 5439–5441.
[52] G.G. Guilbault, S.H. Sadar, R. Glazer, J. Haynes, Anal. Lett. 1 (1968) 333–345.